

Analysis of Losses in Brushless Direct Current Motors and Their Influence upon Operation Characteristics

Monica-Adela Enache, Aurel Campeanu, Ion Vlad, Sorin Enache
University of Craiova, Faculty of Electrical Engineering, Craiova, Romania
menache@em.ucv.ro, acampeanu@em.ucv.ro, ivlad@em.ucv.ro, senache@em.ucv.ro

Abstract - Researches regarding the optimum design and construction of brushless direct current motors are very present, owing to their use in small-dimension vehicles (electrical scooter, electrical bicycle, motor-scooters, electrical vehicles for disabled passengers). Motors used in two-wheel or four-wheel conveyances are permanent magnet direct current motors, manufactured by brushless technology. The operation, starting and speed control characteristics of the brushless direct current motor designed must correspond to certain conditions of competitiveness and to high exigencies imposed by the complex equipments used in passenger-transport vehicles. The study carried out and the simulations presented aim at identifying the important losses in order to reduce them. The widespread use of command electronics associated with power components, in brushless direct current motors supply, enabled the optimization of their operation, with special performances. In this paper there is presented the revised computation relation for iron losses, known in design, by establishing separately the two components: hysteresis losses and eddy-current losses. This way, the efficiency obtained in the design stage gets close to the experimentally established efficiency, the error being less than 2%.

Cuvinte cheie: motoare de current continuu fara perii, proiectare, modelare, simulare.

Keywords: brushless direct current motor, design, modelling, simulation.

I. INTRODUCTION

In recent years, attempts to develop new efficient and clean conveyances have caused an increase in the interest, all over the world, in certain electrical vehicles, having an old or less old history, but the technological level has not enabled their current use so far. An electrical conveyance (bicycle, motor-scooter, Fig.1.a, motorcycle, car, Fig.1), is often presented as an ecological alternative for the traditional mobility.

Use of bicycles/motor-scooters in urban transport [3], [4] was a viable solution many years ago. Low maintenance cost as well as the working agility mattered a lot in a crowded city, the motor-scooter being a very suitable solution. This aspect is only valid if we consider polluting emissions, but a lot of factors have to be analyzed in order to describe a complete image. Brushless direct current motors become attractive in driving conveyances, consequently to the electronics development [1-5], which en-

abled the typified construction of the static commutation devices, characterized by safe use, low cost and small gauge.

Manufacturing an electrical vehicle involves to introduce in the product life cycle [6-7] new materials, as permanent magnets, used in brushless direct current motors or lithium, used in batteries.

This study is carried out in order to have a clearer image of the mobility by electrical conveyances, as an efficient alternative for preserving the environment. Because the cities are more and more polluted, there is the possibility of introducing electrical vehicles as cleaner conveyances. Thus, the XXI-st century conveyances are friendly to the environment, efficient, smart and durable.

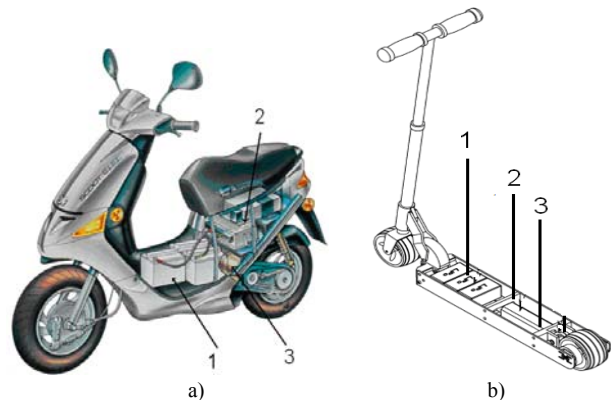


Fig. 1. General view of the driving system (1 –battery, 2- command circuit, 3- brushless direct current motor) for: a) electrical motor-scooter; b) electrical scooter.

There are also differences regarding the breaking technology, energy recovery technology, movement autonomy etc. These specifications are different from one model to another and the main difference consists in the batteries technology.

II. STUDY REGARDING THE LOSSES WEIGHT IN ELECTRICAL MACHINES

A study carried out shows that in low power asynchronous machines, the most used machines in driving systems, the rated load losses [8-11] are distributed as follows: $p_{Cu}=(0.575\div0.645)\cdot\Sigma p$, $p_{Fe}=(0.195\div0.225)\cdot\Sigma p$, $p_{m+v}=(0.115\div0.145)\cdot\Sigma p$, $p_s=(0.050\div0.075)\cdot\Sigma p$. Notations are: p_{Cu} , p_{Fe} , p_{m+v} , p_s –copper losses, iron losses, mechanical and ventilation losses, supplementary losses. In

their turn, the iron losses are divided up into $p_{Fed}=(0.290\div 0.325)\cdot p_{Fe}$, $p_{Fej}=(0.525\div 0.575)\cdot p_{Fe}$, $p_{Fes}=(0.125\div 0.145)\cdot p_{Fe}$ (teeth losses, stator yoke losses, supplementary iron losses).

In the paper proposed, for the same range of power, the same study is carried out for brushless direct current motors, where the rated load losses are distributed as follows: $p_{Cu}=(0.175\div 0.225)\cdot \Sigma p$, $p_{Fe}=(0.625\div 0.705)\cdot \Sigma p$, $p_{m+v}=(0.095\div 0.135)\cdot \Sigma p$, $p_s=(0.020\div 0.035)\cdot \Sigma p$. In their turn, the iron losses are divided up into $p_{Fed}=(0.785\div 0.855)\cdot p_{Fe}$, $p_{Fej}=(0.135\div 0.175)\cdot p_{Fe}$, $p_{Fes}=(0.010\div 0.014)\cdot p_{Fe}$ (teeth losses, armature yoke losses, supplementary iron losses).



Fig.2. View with the magnetic core and the winding in a brushless direct current motor.

It can be noticed that the iron losses prevail in these motors and this aspect will have to be taken into account in designing and choosing the ferromagnetic materials used for the core, Fig.2, in order to increase the energetic efficiency of the motor.

A. Analysis of iron losses in electrical machines

The losses in the magnetic materials used in electrical machines are divided up into two categories:

- Hysteresis losses:

$$p_H = k_H f B_{Fe}^2 m_{Fe} \quad (1)$$

where $k_H=(1.7\div 2.0)$ is a material constant (depending upon the material nature and the magnetization state, f is the frequency and B_m is the amplitude of the iron magnetic induction.

Computing the hysteresis losses is difficult, because of the complex form of the hysteresis cycle and of the dependence upon a lot of factors: frequency, magnetization state, temperature.

- Eddy-current losses:

$$p_F = k_F f^2 B_{Fe}^2 m_{Fe} g_t^2 \quad (2)$$

where k_F is a constant (depending upon the material and the magnetization state).

The relation can be used for magnetic cores made of FeSi hot-rolled laminations, thickness $(0,5\div 0,6)$ mm, electrical conductivity $\sigma_{Fe} = (2\div 2.5)\cdot 10^{-6}$ 1/Ωm.

During punching the lamination, because of the cutting effort the material is forced to, on a depth of round

$(0,4\div 0,6)$ mm along the outline, the cold-hardening phenomenon occurs, where the insulating layer is spoiled. The effect is an increase of the main iron losses. The lamination insulation must accomplish some requirements: to be uniform and compact (without cracks); to be as thin as possible; to have a good elasticity and mechanic resistance; to have high working temperature.

By punching and processing operations made in the magnetic core of electrical machines, the losses increase, $k_d=1.6\div 1.8$, in the teeth, respectively $k_j = 1.25\div 1.4$, in the magnetic core yoke.

In case of magnetic cores made of laminations, the filling coefficient occurs, $k_{Fe}<1$. The value of this coefficient depends upon: the sheet quality, the thickness of the lamination insulation, the quality of the lamination punching, the packing pressing force.

B. Analysis of iron losses

If the field frequency in the magnetic core of electrical machines is high, then a low-gauge machine results, with low weight, low consumption of active material and low manufacturing cost. That is why, brushless direct current motors have a high number of poles and are supplied from batteries by a static converter.

A high weight of the iron losses in these motors causes a lower efficiency. That is why, an optimal design of these motors must take into account not only the low manufacturing cost, but also the working cost. That means to carry out a study regarding the iron losses minimization, which involves separating the hysteresis losses from the eddy-current (Foucault) losses. We solve this problem by using the relation known in books of electrical machines design, for losses:

$$p_{Fe} = p_{10/50} \cdot \left(\frac{f}{50}\right)^{1.3} B_{Fe}^2 m_{Fe} k_{Fep} \quad (3)$$

where: f –frequency, B –magnetic induction, m_{Fe} –iron weight, k_{Fep} – coefficient of losses increase owing to mechanic processing ($k_{Fep}=1.3\div 1.7$).

In the testing bulletin provided by the factory which produces and sells the electro-technical steel sheet used for manufacturing magnetic cores, we find that at $f_1=50$ Hz, $B_1=1.0$ T, the specific losses are $p_{10/50}=2.4$ W/kg, for laminations of $g_t=0.5$ mm thickness.

Without committing a high error, we consider that the specific losses are the same, in a point f_2 , B_2 close to that provided in the testing bulletin of the sheet used. From the design, m_{Fed}/m_{Fea} –teeth/yoke weight and k_{Fed}/k_{Fea} – increase factors of the teeth/stator yoke losses are known.

If we use the iron losses computation relation known in the literature (design), for the two points mentioned above and we compute the stator teeth losses, the result will be:

$$\begin{cases} p_{Fed1} = p_{10/50} \left(\frac{f_1}{50}\right)^{1.3} B_{d1}^2 m_{Fed} k_{Fed} \\ p_{Fed2} = p_{10/50} \left(\frac{f_2}{50}\right)^{1.3} B_{d2}^2 m_{Fed} k_{Fed} \end{cases} \quad (4)$$

The same results are obtained if we compute the teeth losses by using their components: hysteresis losses, respectively eddy-current losses, with the relations:

$$\begin{cases} p_{Fed1} = k_H f_1 B_d^2 m_{Fed} + k_F f_1^2 B_d^2 m_{Fed} g_t^2 \\ p_{Fed2} = k_H f_2 B_d^2 m_{Fed} + k_F f_2^2 B_d^2 m_{Fed} g_t^2 \end{cases} \quad (5)$$

where, the hysteresis losses, p_H , were separated from the eddy-current (Foucault) losses, p_F . If we consider known values p_{Fed1} and p_{Fed2} established with the relation (4), then from (5), by a simple matriceal computation, we establish the coefficients k_H and k_F .

$$X = A^{-1} * B \quad (6)$$

$$A = \begin{pmatrix} f_1 B_d^2 m_{Fed} & f_1^2 B_d^2 m_{Fed} g_t^2 \\ f_2 B_d^2 m_{Fed} & f_2^2 B_d^2 m_{Fed} g_t^2 \end{pmatrix} \quad (7)$$

$$B = \begin{pmatrix} p_{Fed1} \\ p_{Fed2} \end{pmatrix} \quad X = \begin{pmatrix} k_H \\ k_F \end{pmatrix}$$

The coefficients k_H and k_F thus established enable a correct computation of the teeth losses, p_{Fed} , respectively the stator yoke losses, p_{Fea} , for different frequencies and induction:

$$\begin{cases} p_{Fed} = k_H f B_d^2 m_{Fed} + k_F f^2 B_d^2 m_{Fed} g_t^2 \\ p_{Fea} = k_H f B_a^2 m_{Fea} + k_F f^2 B_a^2 m_{Fea} g_t^2 \end{cases} \quad (8)$$

III. SIMULATIONS AND RESULTS

The results obtained and the simulations presented are emphasized in a concrete example of a permanent-magnet brushless direct current motor. The motor operates at low speed and is a reverse construction that meaning exterior inductor, which is the moving part (rotor) and interior armature, which is the stationary part (stator).

The motor is rated as follows: $P_N=100$ W; $U_N=20$ V; $I_N=6.03$ A, $n_N=450$ r.p.m and is manufactured with 27 slots, $2p=30$ NdFeB type magnetic poles. From the design data we have: $g_t=0.5$ mm –lamination thickness, $m_{Fed}=1.682$ kg –teeth weight, $k_d=1.62$ – factor of teeth losses increase, $m_{Fea}=0.553$ kg –yoke weight, $k_a=1.35$ – factor of yoke losses increase, quantities used in the determinations and simulations below.

A. Simulations for establishing the iron losses

On the basis of the mathematical model presented before, for the two operation situations characterized by: $f_1=50$ Hz, $B_1=1.0$ T and $f_2=45$ Hz, $B_2=0.9$ T, considering the same specific losses $p_{10/50}=2.4$ W/kg, the teeth losses have been computed (5). By using the relation (7) there have resulted: $k_H=0.0333/$ $k_F=0.00121$ -factors of proportionality for hysteresis/eddy-current losses. We obtain the same result if we take into account the stator yoke losses.

On the basis of these results there have been carried out some simulations presented in the following figures, which proves that the separate computation of the losses (hysteresis and eddy-current losses) is necessary, Fig.3, in order to obtain correct results.

In Fig.4.a there are plotted curves which show the teeth losses variation relatively to the field frequency, when different computation relations are used:

p_{Fed} –computed with the design relation we know:

$$p_{Fed} = p_{10/50} \left(\frac{f}{50} \right)^{1.3} B_d^2 m_{Fed} k_{Fed} \quad (9)$$

respectively p_{Fe}^* –the same teeth losses, but by using the revised relation

$$p_{Fed}^* = k_H f B_d^2 m_{Fed} + k_F f^2 B_d^2 m_{Fed} g_t^2 \quad (10)$$

In Fig.4.b we have the same curves but for the stator yoke iron losses and in Fig.4.c the total iron losses ($p_{Fe}=p_{Fed}+p_{Fea}$).

Using the known relation (3) for iron losses computation in brushless direct current motors means high errors at high frequencies. In Fig.5 and Fig.6 there are presented simulations which show how the Foucault/total losses increase with the frequency, for different lamination thicknesses. Fig.7 presents simulations with the losses variation at $f=100$ Hz relatively to the lamination thickness; it is notices that, if the lamination thickness decreases to half, then the losses also decrease by 50%.

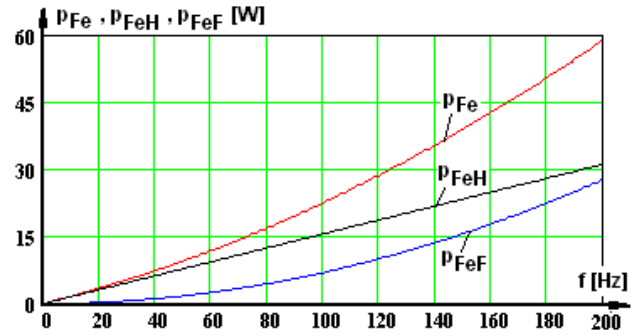
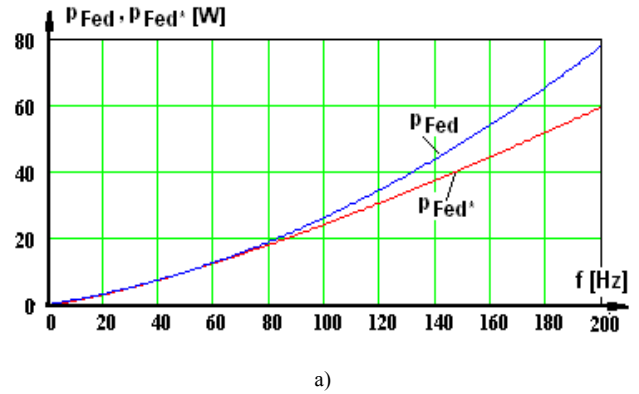
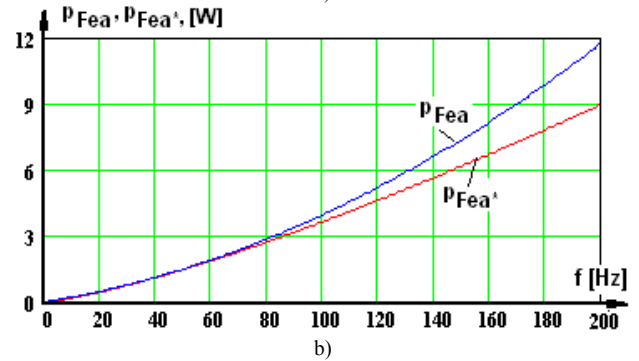


Fig.3. Variation curves of the losses, p_{Fe} hysteresis losses, p_{FeH} and eddy-current losses, p_{FeF} , relatively to the field frequency, for the lamination of $g=0.35$ mm thickness.



a)



b)

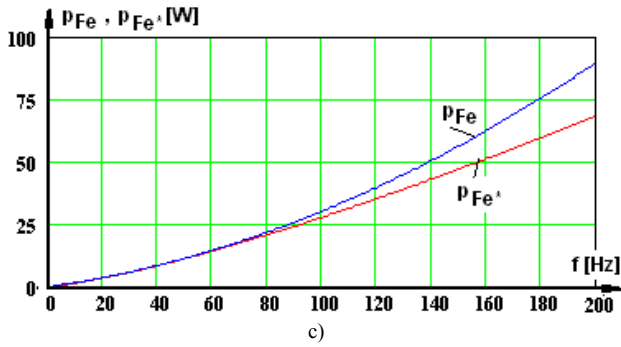


Fig. 4. Variation curves of the losses (p_{Fe^*}/p_{Fe} – losses computed according to the literature/ revised) relatively to the magnetic field frequency, for the lamination of $g=0.5$ mm thickness: a) teeth losses p_{Fe} ; b) stator yoke losses p_{Fe^*} ; c) total iron losses, p_{Fe} .

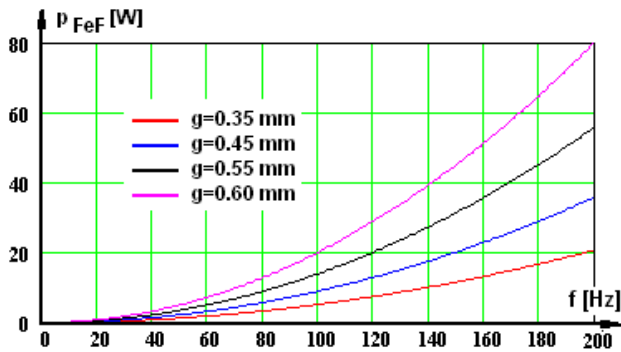


Fig. 5. Variation curves of the eddy-current iron losses relatively to the magnetic field frequency, for different thicknesses of the lamination.

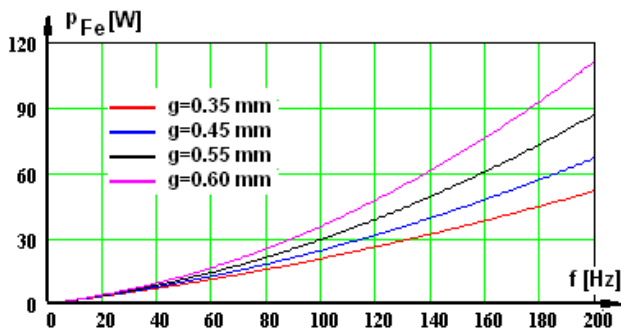


Fig. 6. The variation curves of the total iron losses relatively to the magnetic field frequency, for different thicknesses of the lamination.

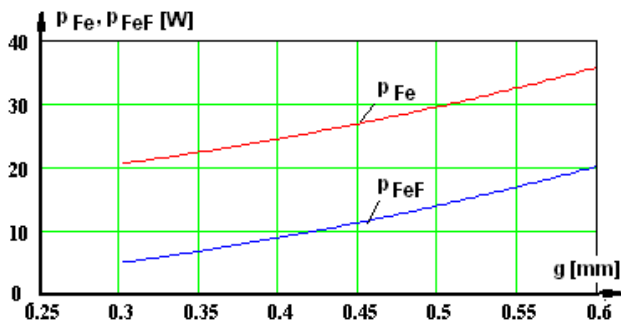


Fig. 7. Variation curves of the iron losses, p_{Fe} and eddy-current losses, p_{FeF} , relatively to the lamination thickness, at a frequency of $f=100$ Hz.

The numerical computation program [12-15] is based on the mathematical model and the simulations carried out and the results obtained allow us to establish a lot of conclusions regarding the iron losses decrease, which are preponderant in brushless direct current motors.

Thus, we have the possibility to minimize the iron losses, in order to result an optimum motor as regards the operation cost, too.

IV. EXPERIMENTAL RESULTS

For such a motor we have in our laboratory, there have been carried out a series of experimental determinations, Fig. 8, which emphasize the accuracy of the simulations and the justifications presented.



Fig. 8. View regarding the experimental determinations.

In the first test, the machine operated as a no-load generator, the mobile armature being driven by a motor with $n=190$ r.p.m. By means of a data acquisition system, the sinusoidal curve of the voltage between two phases has been plotted, Fig. 9 and the fact that they are a symmetrical three-phase system has been emphasized.

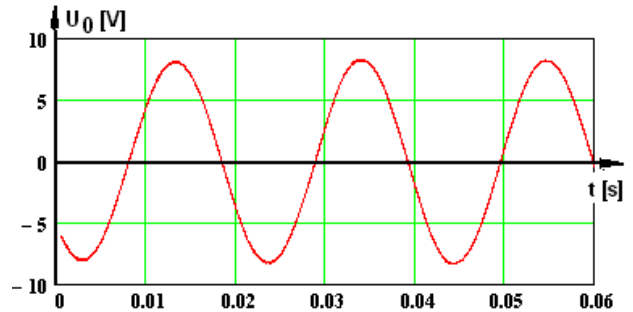


Fig. 9. Line voltage curve at no-load operation as a generator.

The second test was a no-load operation as a brushless direct current motor, with variable supply frequency and voltage (the control device is programmed this way). By using the acquisition system, there have been measured I_0 – input current, P_{10} – power taken from the source, n – speed. The curve of the current I_0 is plotted in Figure 10.

There have been computed p_{Cu} – copper losses, p_c – static converter losses, p_{Fe} – iron losses with the revised relation and, by difference, $p_{m,ex}$ – mechanical losses experimentally established result.

All these curves are plotted in Figure 11. These determinations were necessary in order to establish correctly the locking torque (at starting), where $p_{m,0}=1.82$ W. The mechanical losses can also be computed with analytical relations known in literature,

$$p_m = p_{m0} + 11.5 \cdot \left(\frac{n}{1000}\right)^2 \cdot \left(\frac{D}{100}\right)^4 \quad (11)$$

For different speeds, it is possible to simulate the variation curve of the mechanical losses p_m relatively to speed, which is then compared, in Figure 12, to the curve which was experimentally established $-p_{m,ex}$.

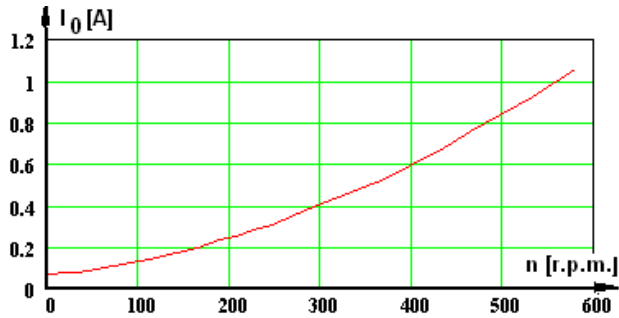


Fig.10. Current curve at no-load operation as a motor when the voltage is variable.

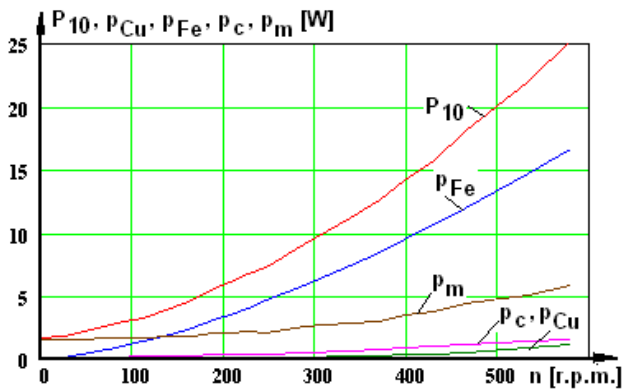


Fig.11. Motor losses at no-load operation with variable voltage: P_{10} – input power, p_{Fe} , p_{Cu} , p_m – iron, copper, mechanical losses.

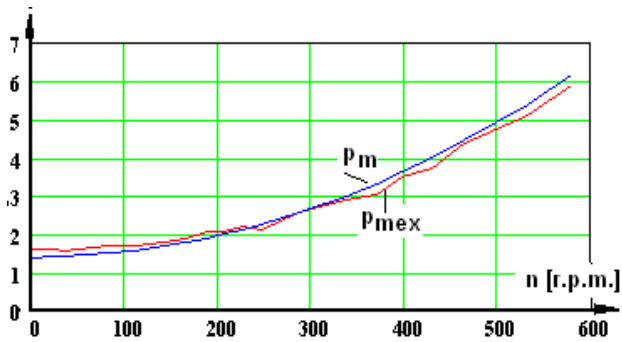
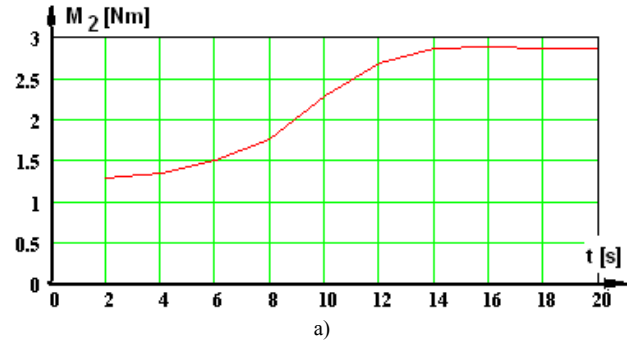


Fig.12. Mechanical losses curves relatively to speed: p_m – computed, p_{mex} – established.

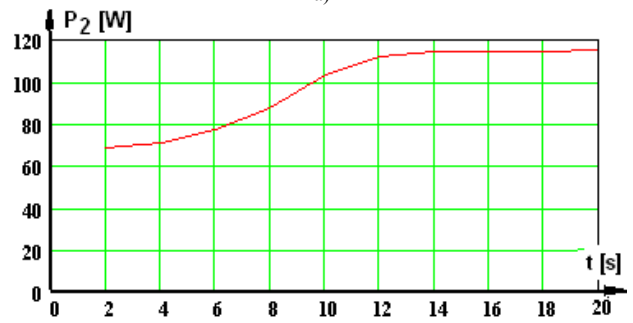
A. Experimental determinations by using the data acquisition system

In the experimental circuit there are voltage, current and speed transducers, which send signals to a data acquisition board -KPCI 3102 – with high speed analogical and digital interfaces, assembled inside the computer. With the circuit from Figure 10 and the acquisition system there have been carried out measurements for voltage, current, torque and speed, for a load increasing up to $M_2=1.4 \cdot M_N=3.0$ Nm.

With these quantities, there have been plotted the graphics: $M_2=f(t)$ –Fig.13.a and $P_2=f(t)$ –Fig.13.b. The two graphics have been used and the time variable has been removed; this way, there has been obtained, through a few points, the torque characteristic, $M_{a,d}=f(P_2)$, for the motor we analyzed, Fig.14.



a)



b)

Fig.13. Curves obtained for an increasing load: a) useful mechanical torque, b) useful power.

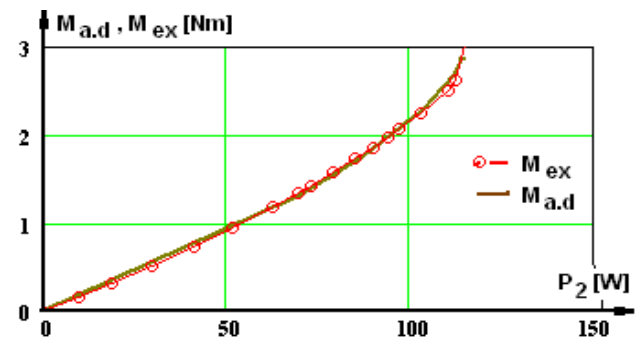


Fig.14. Curves of variation with load for torques: $M_{a,d}$ –curves obtained by simulation and M_{ex} -experimental.

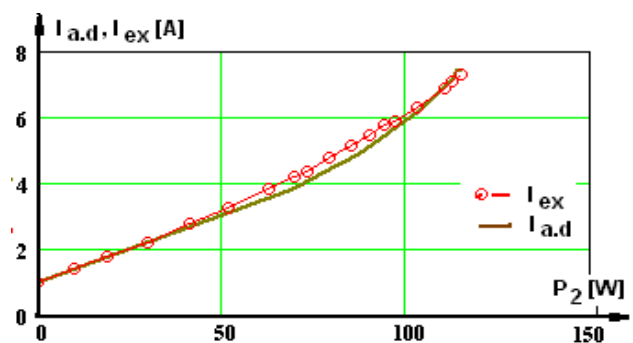


Fig.15. Curves of variation with load for currents: $I_{a,d}$ –curves obtained by data acquisition and I_{ex} -experimental.

Similar graphics have been plotted for: current – Fig.15, speed- Fig.16. In these graphics we have two curves: characteristic obtained with the acquisition system –red colour with dots and the simulated characteristic according to [14], plotted with brown.

The graphics plotted in Figure 17 have been obtained with the data acquisition system, too, where we have the variation curves of the torque and of the current, at rated load, $I_N=6.03$ A. The current curve, Figure 17.b, is almost

trapezoidal (as in case of d.c. machine); as for the torque, Figure 17.a, a lot of low-amplitude oscillations overlap to the continuous component. The high inertia of the rotor generally reduces these oscillations much. From the rated data a torque $M_N=2.15$ Nm results, value closed to the value experimentally established, $M_{2ex.med}=2.194$ Nm (Fig.17.a).

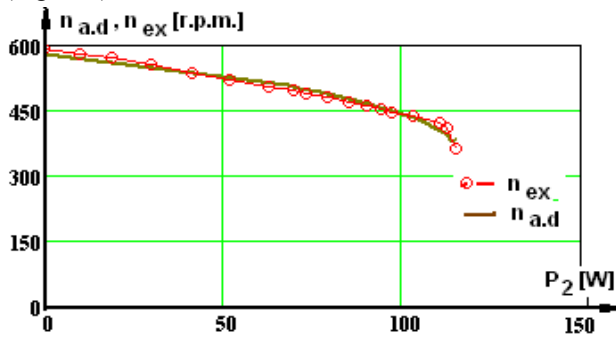


Fig.16. Curves of variation with load for speed: $n_{a.d}$ –curve obtained by data acquisition and n_{ex} -experimental.

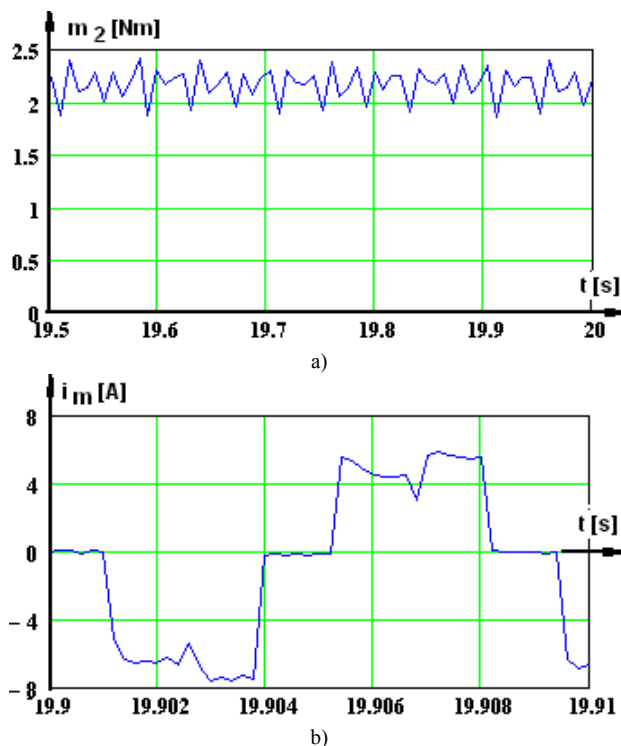


Fig.17.Torque and current curves obtained with the acquisition system at rated load.

CONCLUSIONS

The magnetic core losses in brushless direct current motors can reach (25÷45)% of the total losses, because the magnetic field frequency is high, (100÷250) Hz.

Because of these problems, laminations having a thickness smaller than 0,35 mm, with a percent of silicon of 3,25%, are proposed; after thermally processing the laminations, they get better features: 1,2 W/kg at 60 Hz and 1T, respectively 28 W/kg at 800 Hz and 1T.

The pressing force of the laminations is limited because the main iron losses and the mechanical stresses increase in the consolidation elements of the core. Lacking commutator and replacing it with a static switch,

makes this motor competitive with alternating current motors, by constructive simplicity, operation safety, very low noise, high efficiency, high speed.

The increasing demand of brushless direct current motors, having very low, low and middle power, has impelled the research for finding new materials, with lower losses.

ACKNOWLEDGMENT

This paper was realized under the frame of the grant POC 59/05.09.2016, ID: P_40_401, SMIS 106021.

Contribution of authors:

Firs author – 55%;

Second coauthor – 15%;

Third coauthor – 15%;

Fourth coauthor – 15%.

Received on July 17, 2018

Editorial Approval on November 15, 2018

REFERENCES

- [1] W.C. Chi, M.Y. Cheng, C.H. Chen, "Position-sensorless method for electric braking commutation of brushless DC machines", *IET Electric Power Applications*, Vol.7, Issue 9, 2013, pp.701-713.
- [2] L. Dosiek, P. Pillay, "Cogging Torque Reduction in Permanent Magnet Machines", *IEEE Trans. On Industry Applications*, vol. 43, no. 6, 2007, pp 1565-1571.
- [3] W. Fei, P.C.K. Luk, "A New Technique of cogging Torque Suppression in Direct-Drive Permanent-Magnet Brushless Machines", *IEEE Trans. on Industry Applications*, vol. 46, no. 4, July/August 2010, pp. 1332-1340.
- [4] J. Kaňuch, Z. Ferková, "Design and simulation of disk stepper motor with permanent magnets", *Archives of Electrical Engineering*, vol. 62, no. 2 (2013), pp. 281-288.
- [5] T. Koch, A. Binder, "Permanent magnet machines with fractional slot winding for electric traction", *International Conference on Electrical Machines, ICEM 2002*, Brugge, Belgium, 2002.
- [6] *** Catalogue ICPE Bucharest, Sintered magnets Al-Ni-Co and Nd-Fe-B –magnetic characteristics.
- [7] ***http://www.icpe-me.ro/motoare_magnetii_permanenti.htm
- [8] O. Cira, Lessons of MathCad, The Blue Publishing House, Cluj-Napoca, 2000.
- [9] P. Năslău, R. Negrea, s.a., Computer aided mathematics, Timișoara, Politehnica Publishing House, 2005.
- [10] T. Tomescu, G. Tomescu, Numerical modelling of electromagnetic field, Bucharest, MATRIX ROM, 2004.
- [11] I.A. Viorel, D.M. Ivan, Numerical methods with applications in electrical engineering, Publishing House of University of Oradea 2000.
- [12] T. Sebastian, S. Mir, M. Islam, "Electric Motors for Automotive Applications", *EPE Journal*, vol. 14, no.1, 2004, p.31-37.
- [13] M.A. Enache, A. Campeanu, I. Vlad, S. Enache, Use of Numerical Methods in Computation of Operation Characteristics for Brushless Direct Current Motors, *International Conference on Applied and Theoretical Electricity ICATE 2018*, pp.1-6,.
- [14] S. Enache, A. Campeanu, I. Vlad, M.A. Enache, Numerical Modelling and Torque Analysis in Brushless Direct Current Motors, *XXIII th International Conference on Electrical Machines (ICEM'2018)*, September 3-5, 2018, Alexandroupoli, Greece.
- [15] Y.L. Zhang, W. Hua, M. Cheng, G. Zhang, X.F. Fu, "Static Characteristic of a Novel Stator Surface-Mounted Permanent Magnet Machine for Brushless DC Drives", *38th Annual Conference on IEEE-Industrial-Electronics-Society (IECON 2012)*, 2012, pp.4139-4144.